A Case History of Dynamic Compaction Evaluation by the SASW Method.

by

K. O. Addo[1], M.J. Kokan[1], D. J. Woeller[1], N. F. Beaton[2] and J. O'Brien[3]

Abstract

The evaluation of dynamic compaction should ideally be fast to reduce equipment downtime, produce results in the field for immediate assessment, require neither drilling nor penetration (and so avoid the need for grouting which if improperly done creates potential sources of weakness), be flexible enough to investigate any zone of interest and directly measure properties that are being improved as a function of depth without recourse to empirical correlations. The advent of new heavy-duty placement trucks and deep compaction equipment makes it necessary to develop procedures capable of evaluating lifts much thicker than the traditional 6 to 12 inch specification. The Spectral Analysis of Surface Waves (SASW) is an emerging in-situ testing technique that potentially offers all of the above advantages.

The test is based on the dispersion of Rayleigh-waves which means that Rayleigh waves of different wavelengths propagate at relatively different depths. If the medium of propagation is vertically inhomogeneous, then the different wavelengths propagate at different phase velocities. This variation of phase velocity with wavelength is called a dispersion curve and is related to the structural stiffness of the medium of wave propagation. This paper presents the results of an evaluation of a dynamic compaction project on southern Vancouver Island using the SASW method.

Introduction

As a ground improvement technique, dynamic compaction is aimed at enhancing the stiffness and strength of the target ground. Such improvement, if successfully achieved, limits settlement and reduces foundation size and depth. The method requires repeated application of impacts of massive (approximately 10-25 tonnes) steel or concrete tampers from elevations of about 10-30 metres above the treatment surface. Impact points are predetermined in the treatment area and are cycled through in a specific pattern until the desired improvements are achieved. Under favourable conditions, the mechanism of improvement is a structural rearrangement of the particles in the matrix caused by direct compression and the propagation of stress waves generated by the impact. The process of ensuring that the desired strength or stiffness is achieved is generally referred to as evaluation or control. Details of the dynamic compaction technique have been discussed by Dumas and Beaton (1992).

Existing techniques for evaluating improvements by dynamic compaction are based on the change in resistance to penetration or expansion and include the standard penetration test (SPT), Becker density test (BDT), the cone penetration test (CPT), the pressuremeter test (PMT), the dilatometer test (DMT) and the plate load test (PLT). The Spectral Analysis of Surface Waves (SASW) is a non-intrusive in-situ technique that is particularly suited to the evaluation of dynamic compaction. The test measures the

[1]ConeTec Investigations Ltd., 9113 Shaughnessy St., Vancouver B.C. V6P 6R9.
[2]GeoPac West Ltd., 207-615 8th St., New Westminster, B.C. V3M 3S3.
[3]Macleod Geotechnical Ltd., 1451 Marine Drive, West Vancouver, B.C. V7T 1B8.

elastodynamically related to the stiffness of the propagation medium, any significant stiffness change can be directly determined without recourse to empirical correlations. The non-intrusive nature of the SASW test and the fact that it is based on stress wave propagation which is also the mechanism of improvement by dynamic compaction, makes it ideal for evaluation purposes. In addition, the stress waves produced by the impacts can be potentially used in the SASW procedure. The availability of immediate results in the field is also an added advantage.

Jones (1953) used the principles of the SASW method to evaluate ground improvement by vibratory rolling and to assess changes in ground stiffness due to seasonal variations. Heukelom and Klomp (1962) also successfully used a similar wave propagation method to assess changes in stiffness of a runway due to softening by infiltration. Stokoe et al (1987) used the SASW technique to assess dynamic compaction at Jackson Lake Dam in Wyoming. In this paper, only the fundamental principles of the SASW technique and a case history of dynamic compaction evaluation at a site on southern Vancouver Island are presented. For a more detailed geotechnical treatment of the SASW technique, reference may be made to Nazarian & Stokoe (1984), Tokimatsu et al (1991) and Addo & Robertson (1992). The mathematical details of the required formulation are also well established in the geophysical literature e.g. Haskell (1953), Knopoff (1964) and Kausel & Roesset (1981).

The SASW Technique.

The SASW test is primarily based on the phenomenon of surface-wave dispersion and elasticity theory. The procedure consists of the measurement of the in-situ Rayleigh-wave dispersion curve at a given location and the determination of the variation of shear-wave velocity with depth from the measured in-situ dispersion curve. These two components of the technique are described in this section.

Determination of the in-situ Rayleigh-wave dispersion curve

A vertical impact on the ground surface generally produces both compression, shear, Rayleigh and Love waves. Miller and Pursey (1955) demonstrated that about 67% of the total impact energy propagate as Rayleigh waves. In the SASW method, the propagation of these Rayleigh waves are monitored by two seismic receivers stationed at known distances from the impact point. The impact produces a polychromatic signal (i.e. it contains more than one frequency). The key objective is to determine the velocity at which each of the constituent frequencies travels through the medium between the two seismic receivers. The phenomenon of elastic waves of different frequencies propagating at different velocities is called dispersion and occurs in media that are inhomogeneous. Due to stratification, most natural soil sites, road and runway structures fall into this category. As a general rule, waves of high frequency (or short wavelengths) propagate near the impact surface at a velocity related to the stiffness of the near-surface materials while low frequency signals(or long wavelengths) propagate at greater depths at velocities that reflect the material stiffness at that depth. This principle of dispersion is illustrated schematically in Figure 1. Elastic wave analysis shows that particle motion is significant within a depth of one wavelength from the free-surface. The implication is that the propagation velocity of such an excitation is controlled by the elastic properties of the material within this depth and that the longer the wavelength the greater the depth to which particle motion is significant

The two issues that need be addressed are how to determine the constituent frequencies in the impact signal and how to determine the phase velocity at which each frequency component travels from one receiver to the other. The mathematical concepts required to solve these two problems are the fast Fourier transform and spectral analysis. In simple terms, the fast Fourier transform is a mathematical technique that enables the determination of the frequency components in the polychromatic signals measured at the receiver stations. The details of the technique are beyond the scope of this paper and reference may be made to Cooley and Tukey (1965) for further information. Since the distance between the two receivers is known, the travel time of each frequency component is the only unknown in the computation of propagation velocity from equation [1].

$$v_r = \frac{x_2 - x_1}{\Delta t} \qquad [1]$$

where v_r = Rayleigh-wave velocity of a given frequency component,
x_1 = distance from nearer receiver from impact point,
x_2 = distance from farther receiver from impact point,
Δt = travel time between receivers for the same frequency component.

The travel time for each frequency cannot be measured directly and must be indirectly determined from the phase delay of each frequency component using equation [2].

$$\Delta t = \frac{1}{2\pi f}\phi \qquad [2]$$

where Δt = travel time between receivers,
f = frequency of the component,
ϕ = phase delay of the component.

Given any two signals in the time domain, a quick and efficient procedure for determining the phase delay of each constituent frequency is by computing the cross-spectrum of the signals using equation [3].

$$S_{XY}(f) = \overline{S_Y(f).\, S_X^*(f)} \qquad [3]$$

where $S_{XY}(f)$ = cross spectrum of two time domain signals $Y(t)$ and $X(t)$,
$S_Y(f)$ = Fourier transform of $Y(t)$,
and $S_X^*(f)$ = complex conjugate of the Fourier transform of $X(t)$

The cross-spectrum is generally complex and its phase is a function of the desired phase delay with frequency. When initially calculated, the phase delay is wrapped (i.e. is restricted to between $-\pi$ and $+\pi$ radians) and must be unwrapped into a continuous representation format by adding the appropriate integral number of circles. For details of the computation of the cross-spectrum and why its phase equals the phase delay of the signals, refer to Dziewonski et al, (1969) or Addo (1992). Using this procedure, the phase delay (ϕ) in equation [2] can then be determined for each frequency for the computation of the corresponding travel time and phase velocity.

Due to background and other noise, it is important to ensure that the characteristics of the propagation are not unduly influenced by waves not originating from the intended source. The coherence function, defined in equation [4], estimates the signal-to-noise ratio at each frequency and offers a discriminating parameter by which the quality of the monochromatic components can be assessed. It is similar to the correlation coefficient commonly used in regression analysis.

$$K_{XY}(f) = \frac{\overline{S_{XY}(f)}}{\sqrt{\overline{S_{XX}(f)}}\sqrt{\overline{S_{YY}(f)}}} \qquad [4]$$

where $K_{XY}(f)$ = root mean square coherence,
$S_{XX}(f)$ and $S_{YY}(f)$ = the auto-power spectra of the signals $X(t)$ and $Y(t)$ respectively and
$S_{XY}(f)$ = the cross-spectrum of $X(t)$ and $Y(t)$.

Root mean square coherence values are always positive and always have a value between zero and unity. Frequencies with coherence greater than 0.95 may be considered acceptable but it should also be borne in mind that low coherence values could also be due to factors other than noise.

The above computations are so intensive and tedious that most of the signal acquisition and spectral analyses described above had to be done using special dedicated instruments such as the spectrum analyzer (Nazarian and Stokoe, 1984). The advent of powerful and fast microcomputers, recent innovations in spectral analyses and more robust mathematical algorithms have opened the way for the use of software-controlled signal acquisition and analyses. As a result, a computer program has been developed to handle all the signal acquisition and analyses required to produce the in-situ dispersion curve in the field (Addo and Robertson, 1992).

Determination of Shear Wave Velocity.

The process of determining the variation of shear-wave velocity with depth from a given in-situ dispersion curve is called inversion or forward modelling. Three methods of inversion of varying mathematical rigour are more commonly used and are presented in this section.

The first method, which is also the simplest determines the variation of shear-wave velocity with depth by scaling the axes of the in-situ dispersion curve. Depth is obtained from wavelength using equation [5] (Richart et al , 1970) and shear wave velocity is derived from equation [6] (Filipczynski et al, 1966).

$$z = k_z \frac{v_r}{f} \qquad [5]$$

$$v_s = k_v . v_r \qquad [6]$$

where z = depth from impact surface,
f = frequency,
v_s = shear wave velocity,

v_r = Rayleigh-wave velocity,

and $$k_v = \frac{1+\nu}{0.87+1.12\nu}, \qquad [7]$$

ν being Poisson's ratio.

The factor k_z is related to the depth (expressed in units of wavelength) to the centroid of the zone in which Rayleigh-wave particle motion is significant and the factor k_v is calculated from a simplified form of the elasticity relationship between Rayleigh-wave phase velocity and shear-wave velocity in an ideal medium. For most practical purposes k_z and k_v may be assumed to 0.5 and 1.1 respectively. A k_v of 1.1 is based on a Poisson's ratio of 0.33.

This method of inversion works well except for cases where stiff layers adjoin significantly softer layers or *vice versa*. In such cases the shear-wave velocity in these layers determined from the above equations may be in error due to their mutual influences. Satoh et al (1991) presented a modification of this simplified procedure by accounting for the effect of the stiffnesses of adjoining layers. For layers of increasing stiffness and decreasing stiffness respectively, Satoh et al recommended equations [8] and [9] for modifying shear wave velocities computed using the inversion procedure just described.

$$v_{r_n} = \frac{\bar{v}_{r_n} h_n - \bar{v}_{r_{n-1}} h_{n-1}}{h_n - h_{n-1}} \qquad [8]$$

$$v_{r_n} = \frac{h_n - h_{n-1}}{\frac{h_n}{\bar{v}_{r_n}} - \frac{h_{n-1}}{\bar{v}_{r_{n-1}}}} \qquad [9]$$

where $\bar{v}_{r_n}$, h_n = Rayleigh-wave velocity and thickness of a given layer,

and $\bar{v}_{r_{n-1}}$, h_{n-1} = Rayleigh-wave velocity and thickness of underlying layer.

Mathematically, the third inversion procedure is the most rigorous. It assumes the medium of propagation to be equivalent to a stack of homogeneous layers of infinite lateral extent overlying an elastic half-space. For a stack of n layers including the half-space, calculating the dispersion curve involves the solution of a determinantal equation related to a set of $4n-2$ simultaneous homogeneous equations for each wavelength in the in-situ dispersion curve. The boundary conditions for this eigenvalue problem are continuity of displacements and stresses at each layer interface, zero traction at the free surface and negligible wave amplitude deep within the half-space. Using assumed layer thicknesses, mass densities, shear and compressional wave velocities, a theoretical dispersion curve is calculated based on elastodynamics (Haskell, 1953; Kausel and Roesset, 1981). The layer parameters are then manually (Nazarian and Stokoe, 1984) or automatically (Addo, 1992) perturbed for repeated dispersion calculations until the in-situ dispersion curve is satisfactorily matched. At this stage, the parameters of the layers are then equal to the desired field properties. The process of matching theoretical and in-situ Rayleigh-wave dispersion curves falls in the mathematical realm of constrained optimization.

Site Description.

The site was a waterfront fill in southern Vancouver Island. The fill materials at their initial placement densities were fairly loose and required densification treatment before construction could commence. Borehole data are not available at the site but the area is generally known to consist of random fill overlying till which in turn is underlain by a sedimentary bedrock. The choice of ground improvement by dynamic compaction was independently made and SASW among other tests, was selected for compaction control. SASW tests were performed at three locations at the site. For the purposes of this paper, these locations will be generically referred to as locations A1, A2 and A3.

Field Equipment and Procedure

The equipment used for the SASW testing is schematically shown in Figure 2. A microcomputer is equipped with analog-to-digital and direct memory access cards. Two seismic receivers were consecutively placed at spacings of 15, 8, 4, 2, 1, 0.5, 0.2 m, the location of one receiver being fixed at a distance of about 5m from a designated impact point. Elastic stress waves were then generated by the impact of an instrumented mechanical hammer. The impact hammers varied in mass from 0.5 to 70 kg, the heavier hammers being used for long receiver spacings required to monitor signals of long wavelength. Leads from the hammer and receivers transmitted measured signals into an interface control unit and then to a microcomputer where sampling and digitization took place. The interface control unit contains electronic circuitry for power supply, triggering, amplification and anti-alias filtering of the signals prior to sampling.

For each receiver spacing, five or more signals were averaged in the frequency domain, where the phase of the cross-spectrum and coherence were also calculated. The phase delays and receiver spacing were then used to calculate the Rayleigh wave velocities as a function of frequency using equations [1] and [2]. The procedure was repeated for all the spacings listed above. At the end of testing, dispersion points from the individual spacings are combined into a single dispersion curve for that location. The entire procedure is automated in a computer program SASW-DA (Addo, 1992).

Results and Analysis

The field results of the SASW tests at Locations A1, A2 and A3 are the in-situ Rayleigh-wave dispersion curves shown in Figures 3, 4, and 5. In each case, the dispersion curves measured before and after dynamic compaction (DC) are presented. The general trend is that Rayleigh-wave velocities after DC increased with respect to the initial values. The phase velocity increment ranged from about 40% near the surface to a wavelength of approximately 20 metres where changes became insignificant.

Using the simplest inversion approach discussed earlier, the in-situ dispersion curves were converted to shear wave velocity versus depth curves. Inversion was based on the simplified technique using a k_z value of 0.5. and a k_v value of 1.1. The variation of shear wave velocity with depth for all three locations are shown in Figures 6, 7 and 8.

To evaluate the depth to which dynamic compaction was effective, an approximate relationship (equation [10]) reported by Dumas and Beaton(1992) was used.

$$d_{max} = \alpha\sqrt{Mh} \qquad [10]$$

where d_{max} = theoretical depth of influence,
α = coefficient that accounts for soil type, efficiency of the compaction plant and the compaction program
M = mass of tamper in tonnes
h = height of fall in metres.

For a tamper mass of 16.5 tonnes dropping from a height of 23m, the theoretical depth of influence was calculated to be 9.74 m. This influence depth is shown on Figure 9 which also shows the ratio of after-compaction to before-compaction shear (or Rayleigh) wave velocities plotted against depth. These improvement ratios were calculated using equation [11].

$$IR = \frac{v_{r_{after}}}{v_{r_{before}}} = \frac{v_{s_{after}}}{v_{s_{before}}} \qquad [11]$$

where IR = improvement ratio,
$v_{r_{after}}$, $v_{s_{after}}$ = Rayleigh, shear wave velocity after DC,
and $v_{r_{before}}$, $v_{s_{before}}$ = Rayleigh, shear wave velocity before DC.

Discussion

The results of SASW testing before and after DC, for the three locations tested, have been presented in Figures 3 through 5. The SASW system utilized in the testing program provided dispersion curves in real time in the field which themselves can be used to assess ground improvement. In fact earlier work (Jones, 1953; Heukelom and Klomp, 1962) utilizing surface wave propagation as an investigative tool, commonly reported changes in soil stiffness in terms of Rayleigh-wave phase velocity versus wavelength. Both examples by Jones(1953) and Heukelom and Klomp, (1962) respectively demonstrated the extent of ground improvement and softening by measured changes in in-situ Rayleigh-wave dispersion curves.

The corresponding shear-wave velocity versus depth curves shown in Figures 6 through 8 demonstrate the same trend and magnitude of improvement as the in-situ Rayleigh-wave dispersion curves. Hence Rayleigh-wave dispersion curves and shear-wave velocities may be used as indices of improvement. The ratio of the after-compaction to before-compaction velocities (see equation [11]) is shown plotted against depth in Figure 9. This ratio can be used as an improvement index such that all values greater than unity represent improvement as a percentage of the originally measured value. The theoretical maximum depth of influence of DC was calculated from equation [10] and is shown as the horizontal line in this Figure 9. Very good agreement is seen between theoretical and observed depth of improvement for all three sites.

To confirm the applicability of the SASW testing technique for measuring ground improvement, one can compare the observed improvement depth to the maximum depth predicted from theory. It must be noted that Rayleigh-wave velocity constitutes a more basic, direct and quicker parameter for evaluating DC improvement. The erratic changes in some portions of the dispersion and shear-wave velocity curves are indications of the variability of the existing fill material.

The results presented can be used to evaluate the effectiveness of soil improvement by DC and also to test the credibility of this new non-intrusive technique. Many guidelines have already been recommended for evaluation of DC results, based mainly on penetration tests such as the SPT and the CPT. For difficult sites with large boulders and underground obstructions, the BDT has been used. So is there a rationale for using a very low-strain measurement such as shear-wave velocity to evaluate site improvement? The answer is yes, for the following reasons. Shear-wave velocity is controlled by the stiffness of the soil skeleton which is sensitive to the in-situ stress state, porosity, cementation, age, structure and fabric. Many of these parameters affect the results of large-strain tests in the same manner. Hence small-strain tests are equally appropriate for measuring changes in engineering properties of soils (Burland, 1989). Penetration tests have the disadvantage of being sensitive to minor site variability, especially on difficult sites. In the case of fine-grained fill material interspersed with boulders, the latter would have a significant influence on the measured penetration resistance. However, this influence on shear wave velocities determined from the SASW is rather small since relatively large volumes of material are tested. A more factual basis for using SASW-measured parameters for evaluation is the inherent parallel in stress wave propagation between DC and SASW field testing. Both DC and SASW use a vertical impact producing stress waves that propagate away from the source. The DC method relies on stress waves for soil improvement as does the SASW for Rayleigh and shear wave velocity determination. The SASW technique evaluates the bulk stiffness of the soil over a larger volume and is therefore less sensitive to localized variabilities. It is this overall stiffness of the soil skeleton that ultimately controls settlement characteristics.

Aging needs some consideration when reviewing DC results. Considerable strength gains have been observed in granular soils such as clean sands after a period of several months after application of DC (Mitchell and Solymar, 1984; Schmertmann, 1991). While these improvements are not relied upon in practice they can provide a level of conservatism in the post compaction phase of the analysis (Dumas & Beaton, 1992). All three locations were tested on the same day for each of the before and after phases of testing, so that this effect, if perceptible, should be consistent for all three locations.

Conclusions.

A case history of an evaluation of ground improvement by DC using the SASW method has been presented. The predicted depth to which DC was effective was found to be in good agreement with the corresponding depth inferred from the in-situ dispersion curves determined from the evaluation tests. Improvements in Rayleigh and shear wave velocities were measured. These wave velocities may be directly converted into deformation modulus without recourse to empiricism. The observation that the SASW method was effective for evaluating dynamic compaction is not surprising due to the fact that both improvement and evaluating techniques are based on the propagation of stress waves over relatively long distances.

The relative speed of the test and the simplicity of the required field equipment make the SASW test cost-effective.

Acknowledgments

The authors gratefully acknowledge the invaluable assistance of Macleod Geotechnical Ltd., Bosa Development Corporation and Adara Systems Ltd. of Vancouver, BC. The support of the National Research Council and the Industrial Research Assistance Program (IRAP) is also appreciated.

References

Addo, K.O. 1992. Development of a computerized SASW technique. Ph.D. Dissertation, University of Alberta, Edmonton, Alberta, 271 pp.

Addo, K.O. and Robertson, P.K. 1992. Shear-wave velocity measurement of soils using Rayleigh waves. Canadian Geotechnical Journal, Vol. 29, No. 4, pp. 558-568.

Burland, J.B. 1989. "Small is beautiful" - the stiffness of soils at small strains. Ninth Laurits Bjerrum Memorial Lecture, Canadian Geotechnical Journal, Vol. 26, No. 4, pp. 499-516.

Cooley, J.W. and Tukey, J.W. 1965. An algorithm for the machine calculation of complex Fourier series. Mathematics of Computation, Vol. 19, pp. 297-301.

Dumas, J.C. and Beaton, N.F. 1992. Dynamic compaction, suggested guidelines for evaluating feasibility - for specifying - for controlling. 45th Canadian Geotechnical Conference, Toronto, Canada, Paper No.54, 12 pp.

Dziewonski, A., Bloch, S and Landisman M. 1969. A technique for the analysis of transient seismic signals. Bulletin of the Seismological Society of America, Vol. 59, pp. 427-444.

Filipczynski, L., Pawlowski, Z. and Wehr, J . 1966. Ultrasonic methods of testing materials. Butterworths, London, UK.

Haskell, N.A. 1953. The dispersion of surface waves on multi-layered media. Bulletin of the Seismological Society of America, Vol. 43, pp. 17-34.

Heukelom W. and Klomp J.G. 1962. Dynamic testing as a means of controlling pavements during and after construction. Proceedings of the International Conference on Structural Design of Asphalt Pavement, Ann Arbor, Michigan, pp. 667-679.

Jones, R. 1953. In-situ measurement of the dynamic properties of soil by vibration methods. Geotechnique, Vol. 8, pp. 1-21

Kausel, E. and Roesset, J.M. 1981. Stiffness matrices for layered soils. Bulletin of the Seismological Society of America, Vol. 71, No. 6, pp. 1743-1761.

Knopoff, L. 1964. A matrix method for elastic wave problems. Bulletin of the Seismological Society of America, Vol. 54, No. 1, pp. 431-438.

Miller, G. F. and Pursey, H. 1955. On the partition of energy between elastic waves in a semi-infinite solid. Proceedings of the Royal Society of London, Series A, Mathematical and Physical Sciences, Vol. 233, pp. 55-59.

Mitchell, J. K. and Solymar, Z.V. 1984. Time-dependent strength gain in freshly deposited or densified sand. Journal of Geotechnical Engineering, ASCE, Vol. 110, No. 11.

Nazarian S. and Stokoe (II), K.H. 1984. In-situ shear wave velocities from spectral analysis of surface waves. Eighth World Conference on Earthquake Engineering, Vol. III, pp. 31-38.

Richart, F.E., Hall, J.R. and Woods, R.D. 1970. Vibrations of soil and foundations, Prentice Hall Inc., New Jersey.

Satoh, T., Yamagata, K., Poran, C.J. and Rodriguez, J.A. 1991. Soil profiling by spectral analysis of surface waves. Proceedings of the Second International Conference on Recent Advances in Geotechnical Earthquake Engineering and Soil Dynamics, St. Louis, Missouri, Paper No. 10.23, pp. 1429-1434.

Schmertmann, J.H. 1991. The mechanical aging of soils. 25th Terzaghi Lecture, Journal of Geotechnical Engineering, ASCE, Vol. 117, No. 9,pp.1281-1330.

Stokoe, K.H. II, Roesset, J.M., Nazarian, S., Rix, G.J., Mok, Y.J., Sanchez Salinero, I. and Sheu, J.C. 1987. In situ testing of hard to sample soils. XII Conferenza di Geotecnica di Torino, pp. 1-60

Tokimatsu, K., Kuwayama, S. and Tamura S. 1991. Liquefaction potential based on Rayleigh wave investigation and its comparison with field behaviour. Second International Conference on Recent Advances in Geotechnical Earthquake Engineering and Soil Dynamics, St. Louis, Missouri, Vol. 1, pp. 357-364.

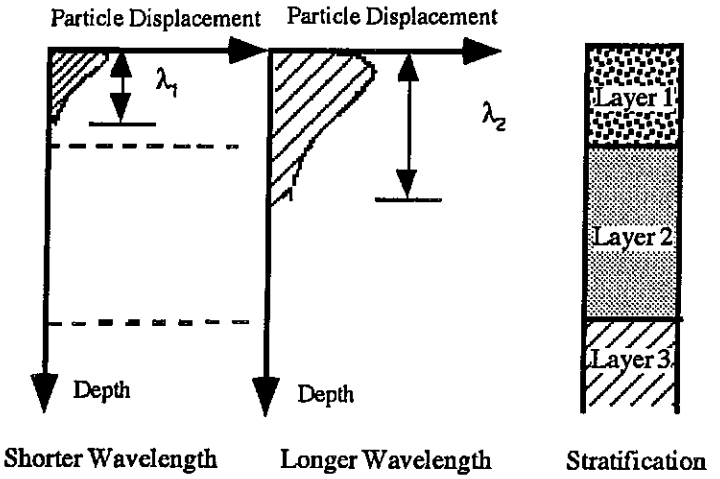

Figure 1. Particle displacement in a medium propagating Rayleigh waves.

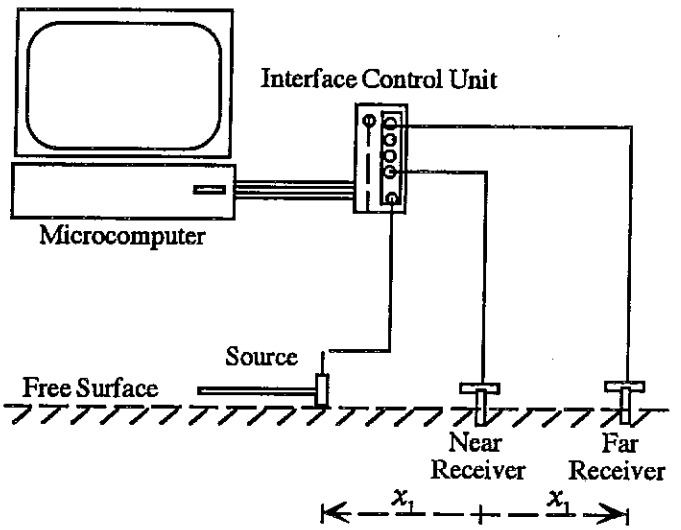

Figure 2. Schematic setup of the SASW Equipment..

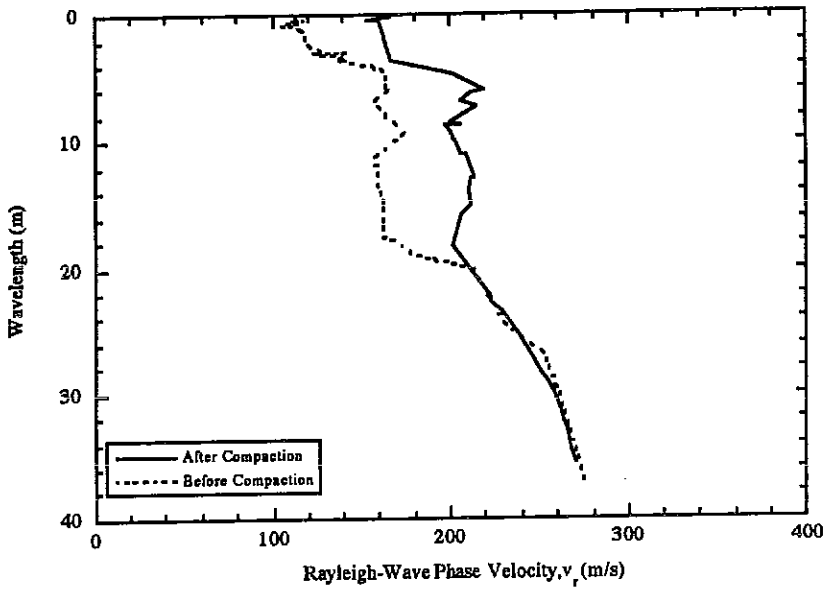

Figure 3. Rayleigh-wave dispersion curves before and after DC at Location A1.

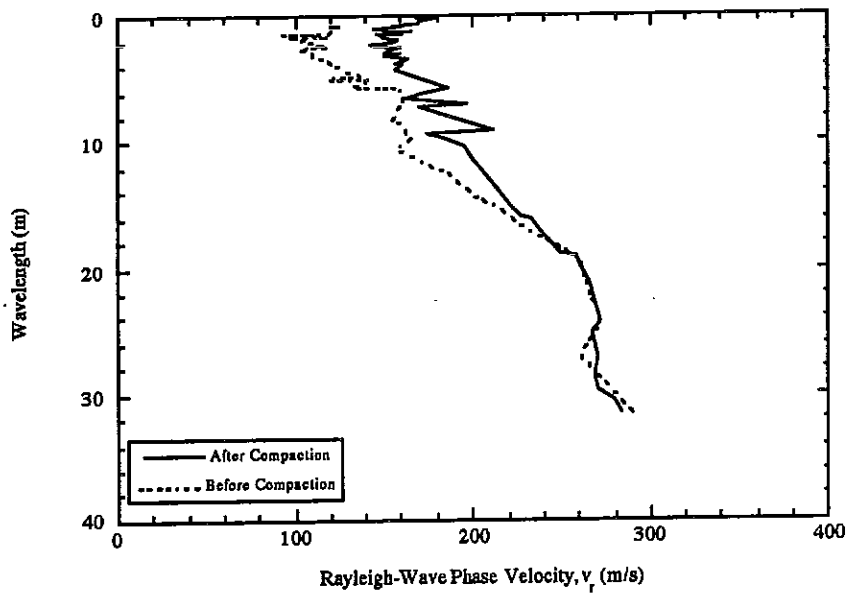

Figure 4. Rayleigh-Wave Dispersion Curves before and after DC at Location A2.

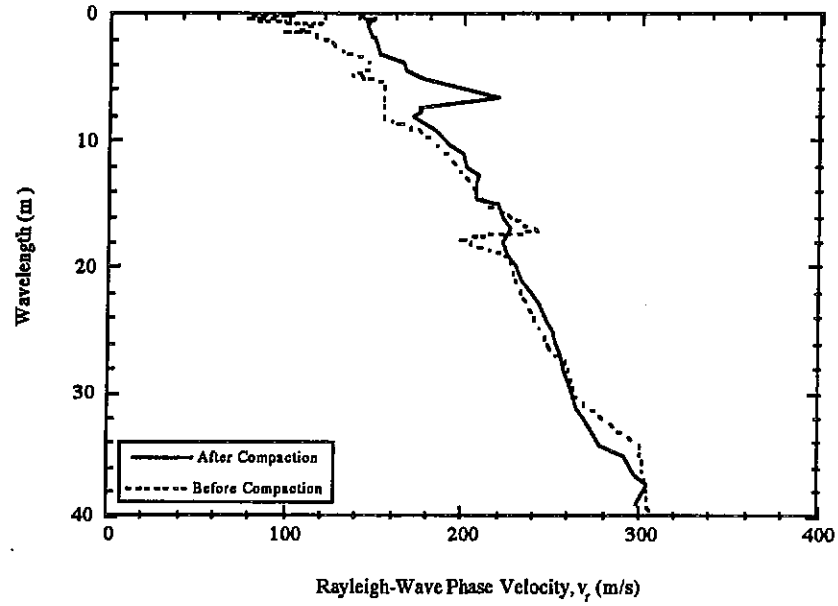

Figure 5. Rayleigh-wave dispersion curves before and after DC at Location A3.

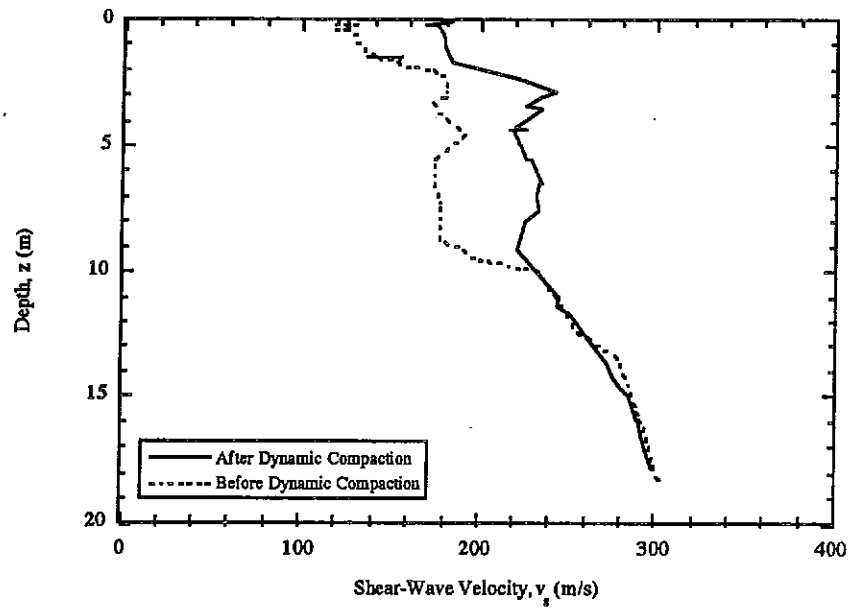

Figure 6. Shear-wave velocity vs. depth before and after DC at Location A1.

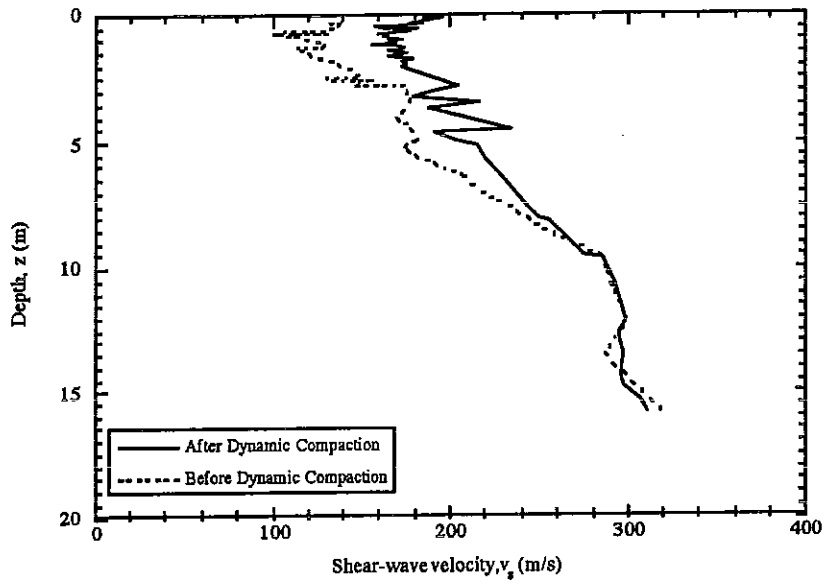

Figure 7. Shear-wave velocity vs. depth before and after DC at Location A2

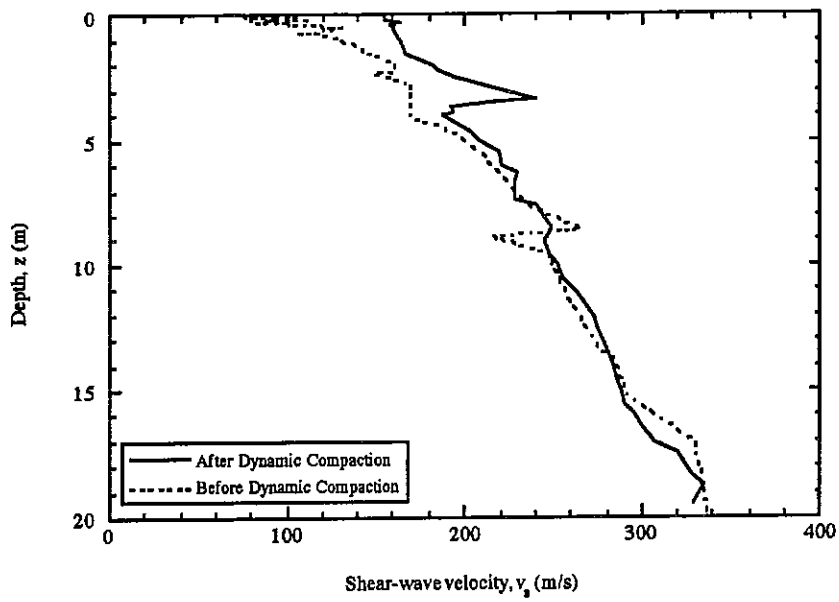

Figure 8. Shear-wave velocity vs. depth before and after DC at Location A3

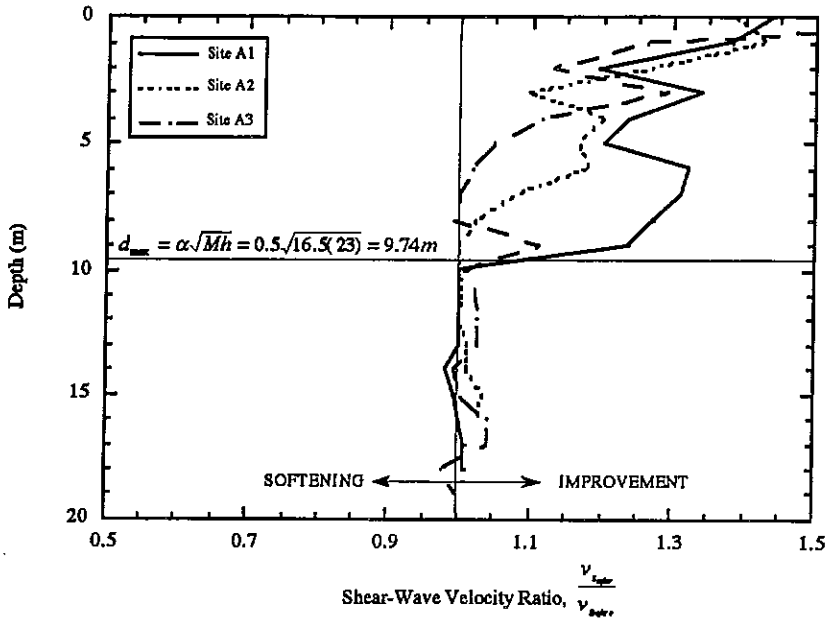

Figure 9. Evaluation of Improvement by Dynamic Compaction.